Insular Cortical Thinning and Altered Structural Connectivity in Chronic Cannabis Users: A High-Resolution Morphometry and Diffusion Tractography Study

Fouad Meraji Far
Alzahra University Hospital, Isfahan University of Medical Sciences
Hamid Reza Banafshe
Kashan University of Medical Sciences
Amir Ghaderi
Kashan University of Medical Sciences
Mohammad Ali Atlasi
atlasima@gmail.com

Kashan University of Medical Sciences
Nassim Jalilvand
Kashan University of Medical Sciences
Rouhollah Sarollahi
Kashan University of Medical Sciences

Research Article

Keywords: Insula, Cannabis, Magnetic Resonance Imaging, Diffusion Tensor Imaging, Addiction

Posted Date: June 18th, 2026

DOI: https://doi.org/10.21203/rs.3.rs-9801898/v1

Additional Declarations: No competing interests reported.

Abstract

Background

The insula, a central hub of the salience network, is implicated in craving and loss of control in addiction. Despite its relevance, the structural morphometric and white matter connectivity correlates of chronic cannabis use remain inconsistent across studies.

Methods

Twenty-six all-male participants (13 chronic cannabis users, 13 controls) underwent a 3.0 Tesla MRI. Cortical thickness and volume were quantified using the Yale Brain Atlas (YBA-696) parcellation. Subcortical volumes were extracted via FreeSurfer. Insula-targeted probabilistic tractography (MRtrix3/iFOD2) was used to assess white matter microstructure through fractional anisotropy (FA), mean diffusivity (MD), axial diffusivity (AD), and radial diffusivity (RD). Group differences were tested with general linear models and Benjamini–Hochberg FDR correction.

Results

Cannabis users showed bilateral insular cortical thinning at whole-insula and parcel levels (eight parcels surviving FDR correction), without volumetric loss. Additional structural differences included reduced total gray matter volume and lower volumes in the brainstem, left amygdala, right thalamus, left cerebellar cortex, and right orbitofrontal gyrus. Tractography revealed reduced diffusivity in left insula–amygdala pathways, lower FA in right insula–hippocampus and right insula–precentral gyrus connections, and reduced FA in left insula–occipital pathways.

Conclusion

Chronic cannabis use is associated with focal insular thinning and selective microstructural alterations in insula–limbic and insula–cortical pathways. These findings support an endocannabinoid-linked vulnerability model in which circuits subserving salience, interoception, and affective valuation are preferentially disrupted, potentially contributing to the transition toward compulsive use.

Introduction

Cannabis remains the most widely used controlled drug worldwide, with global consumption reaching an estimated 244 million people in 2023.(1) Since the World Health Organization's 2020 reclassification of the substance, global prevalence has increased significantly, highlighting a growing need to understand the neurobiological consequences of chronic use.(2, 3) Chronic consumption often leads to cannabis use disorder, a state characterized by a loss of self-control and the persistence of drug-seeking behavior

despite negative consequences(4, 5). Central to these addictive processes is the salience network, which distinguishes salient environmental cues to engage perceptual, emotional, and cognitive modules (6, 7).

The insula is considered the hub of this network, providing the physiological basis for the "self" and integrating interoceptive and proprioceptive arousal.(8, 9) In the context of addiction, the insula mediates craving and the lack of self-control observed in users struggling with drug-related cues.(8–11) The importance of this region is most concretely demonstrated in stroke cases where insular damage results in the immediate and successful cessation of addiction, as if the circuits associating consumption with pleasure were fundamentally disrupted.(9, 12)

Despite its critical role, the specific impact of chronic cannabis exposure on insular morphology remains the subject of debate. (8) Existing structural magnetic resonance imaging (sMRI) studies have yielded conflicting results, with some confirming and others refuting a negative correlation between cannabis use and insular gray matter volume or thickness. (13–16). These discrepancies likely arise from variations in imaging acquisition, small sample sizes, and the inconsistent handling of comorbidities such as tobacco use or psychiatric disorders (17–19). Furthermore, while functional changes are frequently observed, few studies have explored the structural connectivity and white matter tractography of pathways connecting the insula to other subcortical and cortical targets.(20).

According to the prior studies, the morphology and tractography of people with chronic cannabis use, especially in the insula region, are understudied and convey obscure outcomes. This study aims to help to resolve these ambiguities by investigating both the morphology of the insula and the integrity of its related connectomes in a strictly controlled sample. We utilize high-resolution parcellation to retest existing assumptions regarding insular thinning and use diffusion tensor imaging (DTI) to examine anisotropy and diffusivity indices in pathways connected to the insula. Through this comprehensive approach, we seek to provide evidence for an endocannabinoid-linked vulnerability model of structural alterations in circuits subserving salience and valuation.

Materials and methods

Settings and Subjects

The sample size for comparing two means was determined using the reported mean and standard deviation of insular thickness (21), resulting in a required sample size of 13 for each group. Of the 2,183 participants in a census study on substance use conducted as a prelude to this study (22), 329 expressed willingness to participate in imaging. Among these, 28 were chronic cannabis users, defined as using cannabis at least ten times per month for a minimum of two years as a cut-off. Applying the inclusion criterion of infrequent use (at most once a month) of any substance other than cigarettes and cannabis, and the exclusion criteria – which included a history of hypertension, brain surgery, psychiatric disorders, use of neuropsychiatric drugs, claustrophobia, and metal implant, epilepsy, autism, attempted suicide, self-harm, experience of sexual assault or child abuse – resulted in 5 participants in the chronic cannabis user group and 10 in the no-use group agreeing to participate in imaging. An additional 8 participants for the

first group and 3 for the second group were recruited face-to-face from the city and parks. In both cases, inclusion and exclusion criteria were assessed based on self-report. The first group received a gift ranging from zero to one million Tomans, while the second group received a gift ranging from zero to five hundred thousand Tomans.

Image acquisition

All MRI data were acquired on a 3.0 Tesla Siemens Prisma MRI scanner. High-resolution T1-weighted anatomical images were acquired using a 3D magnetization-prepared rapid gradient-echo (MPRAGE) sequence. Imaging parameters were as follows: repetition time (TR) = 2300 ms; inversion time (TI) = 900 ms; echo time (TE) = 2.98 ms; flip angle = 9°. Images were acquired with an isotropic voxel size of 1.0 × 1.0 × 1.0 mm^3, field of view (FOV) = 256 × 256 mm^2, matrix = 256 × 256, and 176 sagittal slices with no inter-slice gap. Parallel imaging was applied using GRAPPA acceleration (factor = 2). Total acquisition time was approximately 5 minutes. These T1-weighted images served as the anatomical reference for cortical morphometry, subcortical segmentation, and cross-modal registration with diffusion data.

Diffusion-weighted images were acquired using a single-shot spin-echo echo-planar imaging (EPI) sequence. Acquisition parameters were as follows: repetition time (TR) = 7600 ms; echo time (TE) = 89 ms; flip angle = 90°. Diffusion data consisted of 68 axial slices covering the entire brain, with a voxel size of 1.8 × 1.8 × 1.8 mm^3, matrix = 128 × 128, and FOV = 230 × 230 mm^2. Diffusion encoding included: One non-diffusion-weighted image (b = 0 s/mm^2), 60 non-collinear diffusion directions at b = 1500 s/mm^2. Total acquisition time was approximately 15 minutes. To enable correction of susceptibility-induced distortions, two diffusion datasets with opposite phase-encoding directions (anterior–posterior and posterior–anterior) were acquired for each participant. All diffusion scans were acquired using a 20-channel head coil and were visually inspected immediately after acquisition for gross artifacts.

Image analysis

FreeSurfer Reconstruction and Subcortical Volumes

T1-weighted images were processed using FreeSurfer (version 7.8.0) (23) with the standard recon-all pipeline. Processing steps included skull stripping, tissue classification, cortical surface reconstruction, and automated segmentation of subcortical structures. All outputs underwent systematic quality control, including visual inspection of brain extraction, white–gray matter boundaries, and pial surfaces.

Volumes of canonical subcortical structures—including bilateral thalamus, caudate, putamen, globus pallidus, hippocampus, amygdala, nucleus accumbens—and estimated total intracranial volume (eTIV) were extracted using asegstats2table. Subcortical volumes were used as primary morphometric outcomes, while eTIV was included as a covariate in volumetric statistical models.

Cortical Morphometry Using the Yale Brain Atlas

Cortical thickness and cortical volume were quantified using the Yale Brain Atlas (YBA) multimodal parcellation, consisting of 696 cortical parcels.(24) Subject-specific YBA outputs were used to extract parcel-wise thickness (mm) and volume (mm^3).

To maintain conceptual consistency with the insula-centered connectivity framework described by Ghaziri and colleagues (25) and FSL Harvard–Oxford Cortical Structural Atlas (26)YBA parcels were aggregated into anatomically defined macroscopic cortical regions in each hemisphere, spanning frontal, parietal, temporal, occipital, and limbic cortices. Parcel-to-macro-region mapping was implemented using a curated lookup table that assigns each YBA parcel to a macro-region based on anatomical location and prior tractography literature. For each participant, hemisphere, and macro-region, mean cortical thickness was calculated as the average of parcel-wise thickness values. Total cortical volume was computed as the sum of parcel-wise volumes. This macro-level morphometry dataset served as the cortical structural outcomes for group-level analyses.

Diffusion MRI Preprocessing

Diffusion preprocessing was performed using FSL (version 6.0.7.19) (27) and MRtrix3 (version 3.0.8) (28). Raw DICOM images were converted to NIfTI format and organized into subject-specific anatomical and diffusion directories. Susceptibility-induced distortions were corrected using FSL TOPUP, based on paired anterior–posterior and posterior–anterior b0 images. Eddy-current-induced distortions and subject motion were corrected using FSL eddy with outlier replacement and rotation of diffusion gradient vectors. Standard eddy quality-control outputs were inspected for excessive motion and signal dropout. A mean b0 image was generated and skull-stripped using FSL BET to create a diffusion brain mask. Intensity inhomogeneity was corrected using ANTs (29) N4 bias-field correction implemented via MRtrix (dwibiascorrect ants). Diffusion tensors were estimated using MRtrix (dwi2tensor), and scalar diffusion maps—including fractional anisotropy (FA), mean diffusivity (MD), axial diffusivity (AD), and radial diffusivity (RD)—were derived using tensor2metric.

Cross-Modal Registration

High-resolution T1-weighted images were nonlinearly registered to MNI152 (30) 1 mm standard space using ANTs with affine and symmetric diffeomorphic (SyN) transformations. The eddy-corrected b0 image was registered to the native T1 image, and the resulting transforms were inverted to accurately project anatomical and atlas-based ROIs into native diffusion space. Transform concatenation minimized interpolation steps and preserved label integrity.

Parcellation and ROI Definition in Diffusion Space

Cortical and Insular ROIs

The YBA-696 atlas was transformed from MNI space into each participant's diffusion space using nearest-neighbor interpolation. Insular parcels were identified based on YBA anatomical labels and compiled into hemisphere-specific insula ROI sets. Non-insular cortical parcels corresponding to the predefined macro-regions served as cortical targets for connectivity analyses.

Subcortical ROIs

FreeSurfer automated subcortical segmentations (aseg) were resampled into diffusion space via T1-to-DWI transformations. Individual nuclei were binarized and relabeled to generate a compact subcortical ROI volume comprising 14 bilateral structures (thalamus, caudate, putamen, globus pallidus, hippocampus, amygdala, nucleus accumbens), used for insula–subcortical connectivity analyses.

Fiber Orientation Estimation and Tractography

Fiber orientation distributions were estimated using single-shell constrained spherical harmonic deconvolution. A five-tissue-type (5TT) image was generated from the T1-weighted scan and registered to diffusion space to enable anatomically constrained tractography (ACT).

Whole-brain probabilistic tractography was performed using the iFOD2 algorithm with seeding at the gray–white matter interface. Tracking parameters followed MRtrix recommendations for single-shell data, with a step size approximately half the voxel size. For each participant, a whole-brain tractogram containing on the order of 10^6–10^7 streamlines was generated. Structural connectomes were generated using MRtrix tck2connectome. Diffusion metrics were sampled along streamlines and averaged per connection. Whole-brain connectomes were retained for exploratory analyses.

Statistical analysis

Statistical analyses were conducted in R (version 4.5.2). General linear models were used to test group differences, adjusting for age, body mass index, and intracranial volume where appropriate. Streamline counts were log-transformed to reduce skewness. Multiple comparisons were controlled using the Benjamini–Hochberg false discovery rate (FDR) procedure within predefined families of tests ($q < 0.05$). Effect sizes and 95% confidence intervals were reported for all significant findings.

Results

Participant characteristics

Twenty-six all-male participants were included in the final sample (13 cannabis users; 13 controls). Groups were comparable in age and body mass index (Table-1).

Table 1. Participants characteristics

Group	Number	Gender	Age (mean ± SD)	BMI (mean ± SD)	Welch's p
Cannabis	13	All male	24.5 ± 4.7	23.7 ± 3.5	0.510
Control	13	All male	25.7 ± 4.7	25.7 ± 4.7	0.402

Notes: BMI is body mass index, defined as weight per height square in kg/m²; Comparison between groups with Welch Two Sample t-test.

Global brain structure, subcortical and cortical volume

The estimated total intracranial volume did not differ between groups. In contrast, total gray-matter volume was lower in cannabis users (Table 2). Subcortical gray-matter volume showed a similar direction but did not survive correction. No group differences were observed for total cerebral white-matter volume or composite brain segmentation volumes.

Among subcortical and infratentorial structures, cannabis users exhibited lower volumes in the brainstem, left amygdala, right thalamus, and left cerebellar cortex (Table 2). No other subcortical structures survived correction.

For cortical volume, a focal group difference was observed in the right orbital frontal gyrus, with lower volume in cannabis users (Table 2). No other cortical ROI volumes survived FDR correction. For cortical thickness, no ROI survived correction.

Table 2. Whole-brain, cortical, and subcortical volumes (independent-samples t-tests)

Measure	Cannabis (mean ± SD)		Control (mean ± SD)		p	q_FDR
Total gray-matter volume	660906.8	55636.1	694086.6	58823.0	0.036	0.036
Brainstem	19891.2	2006.3	21996.1	1706.3	0.008	0.008
Left amygdala	1716.3	179.7	1861.4	160.4	0.033	0.033
Right thalamus	7843.2	1213.3	8547.6	571.4	0.037	0.037
Left cerebellar cortex	55058.0	7010.5	58312.6	6650.1	0.049	0.049
right orbital frontal gyrus	10006.8	616.1	11388.6	1516.0	0.001	0.035

Notes: Volumes are in mm³; q_FDR is Benjamini–Hochberg correction (alpha < 0.05).

Insular thickness

Whole-insula morphometry showed preserved volume but lower thickness in cannabis users. Insular volumes did not differ between groups. In contrast, mean insular thickness was lower in cannabis users in both hemispheres. The bilateral mean difference in insular thickness was likewise significant. (Table 3)

Table 3. Whole-insula morphometry (independent-samples t-tests)

Measure	Cannabis (mean ± SD)		Control (mean ± SD)		p	q_FDR
Insula volume (Left)	4816.8	550.3	4751.1	447.6	0.741	0.741
Insula volume (Right)	4673.8	565.9	4982.8	1154.3	0.398	0.597
Insula volume (Total)	9490.6	990.4	9733.8	1379.9	0.611	0.733
Insula thickness (Left)	3.062	0.280	3.409	0.196	0.001	0.005
Insula thickness (Right)	3.034	0.295	3.347	0.207	0.005	0.010
Insula thickness (Bilateral mean)	3.048	0.279	3.378	0.173	0.002	0.005

Notes: Volumes are in mm^3; thickness is in mm; q_FDR is Benjamini–Hochberg correction.

At the parcel level (high-resolution insula parcellation), no parcel-volume differences survived FDR correction. In contrast, eight parcels demonstrated lower thickness in cannabis users after FDR correction (Table 4). Across these parcels, thickness reductions were on the order of ~0.30–0.70 mm relative to controls, indicating that the insular effect was expressed predominantly as focal cortical thinning rather than volumetric loss.

Table 4. Insula parcel-wise thickness reductions surviving FDR (linear models; YBA parcels)

Hemisphere	Parcel	Cannabis (mean ± SD)		Control (mean ± SD)		p	q_FDR
Left	L_I1_A	2.88	0.32	3.23	0.29	0.005	0.030
Left	L_I4_A	2.47	0.17	2.77	0.32	0.002	0.014
Left	L_I4_C	3.09	0.44	3.79	0.31	0.000	0.002
Left	L_I5_C	3.01	0.41	3.63	0.40	0.000	0.003
Right	R_I3_A	2.68	0.26	2.98	0.20	0.002	0.014
Right	R_I3_C	3.55	0.64	4.06	0.48	0.009	0.043
Right	R_I4_B	2.78	0.51	3.23	0.39	0.010	0.044
Right	R_I5_B	2.66	0.50	3.32	0.49	0.005	0.030

Notes: Parcel labels correspond to the YBA (figure 1); thickness in mm; q_FDR is Benjamini–Hochberg correction (alpha < 0.05).

Insula–subcortical structural connectivity

Insula–subcortical pathways were quantified using diffusion-derived tract microstructure (FA, MD, AD, RD). Given missing tract estimates for several subcortical targets, ROI-level inference focused on pathways with adequate coverage across participants—most consistently the amygdala and hippocampus (n = 13 per group) and, to a lesser extent, the nucleus accumbens (reduced n in both groups). Group effects were tested using linear models with FDR correction within each hemisphere × metric family.

At the ROI level, the left insula–amygdala pathway showed lower MD in cannabis users (Table 5). No other ROI-level insula–subcortical effects survived FDR correction.

Table 5. Insula–subcortical structural connectivity: group differences (linear models).

Hemisphere		Parcel	Subcortical	Index	Cannabis (mean ± SD)		Control (mean ± SD)		p	q_FDR
1	Left	Whole	Amygdala	MD	0.972	0.050	1.031	0.051	0.014	0.041
2	Left	Whole	Amygdala	AD	1.188	0.044	1.247	0.065	0.019	0.057
3	Left	Whole	Amygdala	RD	0.864	0.056	0.924	0.048	0.018	0.053
4	Left	Whole	Amygdala	FA	0.228	0.030	0.215	0.022	0.413	0.413
5	Left	L_I2_B	Amygdala	FA	0.291	0.059	0.221	0.034	0.001	0.019
6	Left	L_I2_B	Amygdala	MD	0.887	0.033	1.049	0.156	0.008	0.039
7	Left	L_I2_B	Amygdala	RD	0.753	0.054	0.937	0.153	0.003	0.035
8	Left	L_I3_C	Amygdala	AD	1.160	0.079	1.352	0.014	0.006	0.026
9	Left	L_I4_A	Amygdala	MD	0.988	0.098	1.100	0.077	0.006	0.039
10	Left	L_I4_A	Amygdala	AD	1.186	0.087	1.303	0.082	0.002	0.026
11	Left	L_I5_A	Amygdala	MD	0.911	0.096	1.113	0.107	0.004	0.039
12	Left	L_I5_A	Amygdala	AD	1.119	0.103	1.336	0.121	0.004	0.026
13	Left	L_I5_A	Amygdala	RD	0.807	0.097	1.002	0.107	0.005	0.035
14	Right	R_I5_C	Hippocampus	FA	0.234	0.042	0.394	0.073	0.005	0.050

Note. FA is unitless; AD/MD/RD values in $\times 10^{-3}$ mm^2/s; q_FDR is Benjamini–Hochberg correction (alpha < 0.05).

Edge-wise analyses localized group effects to specific insula-parcel–to–subcortical connections (FDR correction within each hemisphere × metric family across tested edges). Within the left insula–amygdala system, cannabis users exhibited (i) higher FA for L_I2_B–amygdala and (ii) lower diffusivity for multiple edges, including reduced AD for L_I3_C, L_I4_A, L_I5_A–amygdala, lower MD for L_I2_B, L_I4_A, L_I5_A–amygdala, and lower RD for L_I2_B, L_I5_A–amygdala (Table 5). In the right hemisphere, a single hippocampal connection showed lower FA in cannabis users R_I5_C–hippocampus (table 5). Notably,

several significant edges were driven by lower per-edge sample sizes due to missing tract estimates, and these findings should be interpreted accordingly.

Left-hemispheric insula–cortical connectivity

Left hemisphere insula–cortical tract microstructure was assessed across cortical targets using both ROI-level connectivity (mean tract metric per cortical target) and an edge-wise analysis of insula-parcel–to–cortex connections. Two cortical targets (pars opercularis and superior temporal gyrus) showed no tract estimates in either group and were excluded.

At the ROI level, analyses identified reduced tract FA between the insula and specific occipital regions after FDR correction: Occipital Fusiform Gyrus – Lateral, Occipital Fusiform Gyrus – Medial, and Lingual Gyrus – Posterior (Table 6). No ROI-level group differences survived correction for diffusivity metrics. Insula parcel–level mean connectivity to occipital ROIs did not reach the corrected threshold. However, edge-wise analyses localized a single left-hemispheric effect to the Insula–Occipital Fusiform Gyrus–Medial connection, with higher RD in cannabis users (Table 6). No additional edge-wise effects survived FDR correction.

Right-hemispheric insula–cortical connectivity

Analogous analyses were performed for the right hemisphere(Figure 2). As in the right hemisphere, the pars opercularis and the superior temporal gyrus had no tract estimates in either group and were excluded. At the ROI level, no group differences survived FDR correction for FA, MD, AD, or RD. At the edge level, a single connection survived FDR correction: FA was lower in cannabis users for the R_I5_A–precentral gyrus edge (Table 6). No edge-wise effects survived FDR for MD or AD. RD was higher for the same edge (Δ = 0.104×10^{-3} mm^2/s; p = 1.61×10^{-4}), but remained subthreshold after correction (qFDR = 0.0659).

Table 6. Insula-cortical structural connectivity: FDR-significant group differences.

Hemisphere	Parcel	Target ROI	Index	Cannabis (mean ± SD)		Control (mean ± SD)		p	q_FDR
Left	Whole	Fusiform lateral	FA	0.434	0.026	0.469	0.021	0.001	0.011
Left	Whole	Fusiform medial	FA	0.444	0.049	0.487	0.017	0.010	0.043
Left	Whole	Lingual posterior	FA	0.468	0.041	0.504	0.023	0.013	0.043
Left	L_I4_A	Fusiform medial	RD	0.666	0.010	0.527	0.001	0.000	0.021
Right	R_I5_A	Precentral gyrus	FA	0.281	0.044	0.359	0.044	0.000	0.050

Note. Parcel labels correspond to the YBA insula parcel ordering used in the morphometry outputs (Figure 1). FA is unitless; AD/MD/RD values in $\times 10^{-3}$ mm^2/s. q_FDR values correspond to Benjamini–Hochberg (alpha < 0.05).

Discussion

Morphology

The key finding of this study is that cannabis users showed bilateral insular thinning, with multiple insular parcels showing focal thickness reductions. However, no parcel-wise differences in insular volume were reported. Reported. This pattern is logical as cortical volume encompasses both thickness and surface area. It is possible for preferential thinning to occur without a discernible loss in volume, particularly with small sample sizes or when changes in thickness and surface area partially offset one another. Our analytic strategy was explicitly insula-centric and used a high-resolution parcellation (YBA-696) with macro-regional aggregation designed to align with modern tractography-informed descriptions of insular organization and connectivity. The lower thickness and preserved volume in the insula can also be explained with the disruption of the structural covariance networks (SCNs) reported previously in young adults with heavy cannabis use and coordinated maturation patterns.(31) Cannabis may interfere with the typical neurodevelopmental pruning or thinning process in the insula, potentially creating a biomarker for the transition to compulsive use.

The broader structural MRI literature on cannabis exposure has been notably heterogeneous, depending on cohort age, dependence status, comorbid substance exposure, and analytic approach. (19, 32, 33). An updated systematic review and meta-analysis by Lorenzetti and colleagues emphasized this heterogeneity. (19). They urged cautious interpretation and highlighted that, when present, effects tend to involve regions densely innervated by cannabinoid receptors and implicated in addiction-related neurocircuitry. (19, 34, 35).

Particularly, a large multisite cortical surface study combining data from four independent cohorts found no significant differences in cortical thickness, surface area, or gyrification between regular cannabis users and controls after adjusting for key covariates, including alcohol and nicotine exposure. (2, 17) Likewise, no differences in thickness were observed when stratifying by dependence status or age of onset. Several non-mutually exclusive factors may explain this apparent discrepancy with our insula thinning. Whole-brain vertex-wise or atlas-level analyses may be less sensitive to focal, parcel-level insular effects. Cannabis-related morphometric changes may be spatially heterogeneous within the insula, so effects are diluted when averaging across larger regions. Sample characteristics such as dependence severity, age of onset, abstinence status, and polysubstance exposure likely influence insular morphology in ways that are not fully harmonized across studies.

We observed a focal reduction in right orbitofrontal gyrus volume in cannabis users. The orbitofrontal cortex (OFC) is a core region involved in valuation, reward learning, and outcome-guided decision-making. It is commonly implicated in addiction models that emphasize altered incentive salience and impaired top-down regulation. Large-scale consortium data from the ENIGMA Addiction Working Group reported that

dependent cannabis users – particularly females – had marginally significantly smaller lateral OFC and cerebellar white matter volumes compared with recreational users and controls (19, 36). In contrast, many other a priori regions, including the insula and amygdala, did not show significant group effects in that sample. Our finding of reduced OFC volume is therefore directionally consistent with the ENIGMA observation that the OFC may be one of the more reliably sensitive cortical targets in cannabis dependence (19). However, the laterality (right OFC in our sample) and the presence of additional subcortical differences emphasize that effect localization may depend on cohort composition and analytic resolution.

We also detected reduced left amygdala volume in cannabis users. The amygdala is central to affective salience, threat learning, and stress responsivity – processes frequently altered in chronic cannabis use and cannabis use disorder (CUD) (18). Although ENIGMA did not detect robust amygdala volume differences at the ROI level in its harmonized analysis, the same study explicitly selected limbic ROIs (including the amygdala, hippocampus, insula, OFC, ACC, and cerebellum) because of their relevance to addiction theories and their high CB1 receptor density (19, 37). The difference between our findings on the amygdala and ENIGMA's lack of effect is probably due to variations in sample size and statistical power, definitions of dependence, gender composition, and the approach to managing comorbidity. Additionally, it underscores a wider observation made in meta-analytic studies indicating that structural effects linked to cannabis are usually subtle, influenced by context, and require methodological consistency. (34, 35).

Robust thinning we observed in specific parcels provides a structural explanation for why cannabis users struggle to switch from internal craving (Default Mode Network or DMN) to cognitive control (Central Executive Network). This structural damage may be the reason for the hypoactivation of the insula during demanding tasks.(38, 39)

We observed reduced volumes in the right thalamus, left ventral diencephalon, brainstem, and left cerebellar cortex, as well as reduced total gray matter volume. These structures are relevant to reward, arousal, sensory integration, and cerebello–thalamo–cortical control loops. The cerebellum, in particular, is frequently discussed in cannabinoid neuroscience because of its high CB1 receptor expression and its role in motor coordination and cognitive timing. ENIGMA's observation of cerebellar involvement, especially in cerebellar white matter, in dependent users is consistent with the broader interpretation that chronic cannabis exposure may alter cerebellar circuitry in a dependence- and sex-contingent manner (13, 19).

Tractography

The insula-targeted tractography analysis, given that the insula is recognized as a highly connected hub for interoceptive, affective, and cognitive-control signals, is a key contribution of the current study. Human tractography studies have shown that the insula has a broad set of cortical connections with a rostro-caudal organization, including connections to frontal (orbitofrontal/prefrontal), cingulate, temporal, parietal, and limbic territories (40). Consistent with prior studies, the insula-subcortical tractography showed solid connectivity with the thalamus, striatum, hippocampus, amygdala, and nucleus accumbens. However, it's worth noting that streamline-derived connectivity measures can be biased by algorithmic and anatomical factors (e.g., tract length, ROI geometry, partial volume), inspiring careful interpretation of tractography-

derived metrics. Against this anatomical background, the present study found that the left insula–amygdala pathway exhibited reduced MD at the ROI level, with edge-wise analyses showing lower MD, AD, and RD for multiple insula parcel–amygdala connections and higher FA in one parcel–amygdala edge (20, 41).

Lower diffusivity and higher FA can indicate various microstructural changes, such as altered axonal packing, myelination, or reduced extracellular water content. However, diffusion tensor metrics are not specific to any single tissue property, and tractography-derived tract averages also reflect streamline selection and crossing-fiber complexity. Therefore, the most defensible interpretation is that chronic cannabis use is associated with altered microstructural organization within this fronto–insular–limbic pathway.

Comparison of these findings with previous DTI studies helps to gain distinct insights. In a diffusion tensor study of young adults (39 cannabis users and 28 controls), Cousijn et al. reported no differences in group-level analysis in white matter microstructure, but found that earlier onset of weekly cannabis use was associated with lower FA in tracts including the uncinate fasciculus, a prototypical fronto-limbic pathway (42). The microstructural alterations caused by cannabis use may be localized within specific fronto-limbic systems. The global evaluations of the white matter do not show these subtle changes. Accordingly, they are more identifiable when analyses target anatomically plausible pathways (as insula-amygdala). (13, 20)

We also detected a right insula-hippocampus edge with reduced FA. The hippocampus is responsible for contextual learning and memory processes, influencing cue reactivity and habit formation in substance use, as the hippocampal circuit network has a significant role in cannabis-related cognitive outcomes. Despite the fact that we did not observe hippocampal volume differences between the groups of the study, insula-hippocampus microstructural alterations may be a representation of an early or indistinct network-level marker that precedes macrostructural change, or a compensatory remodeling that co-occurs with focal cortical thinning. Lower FA in the right insula-hippocampus and higher FA in the left insula-amygdala represent a structural shift that prioritizes cue-induced craving over contextual learning, explaining why users find it difficult to quit cannabis despite adverse effects.(5)

The only affected insula-cortical connectivity was the insula-precentral connection, which had reduced FA and a near-significant increase in RD. The insula has a crucial role in integrating interoceptive signals with motor planning and execution (43), as there is evidence that cannabis can affect sensorimotor performance and motor learning. The relative specificity of this effect – rather than widespread disruption of cortical connectivity – also reflects the broader literature suggesting that cannabis-related white matter alterations, when present, are often modest, regionally selective, and may depend on developmental timing and exposure severity (35).

There is also a left-lateralized pattern of insula–occipital microstructural differences. At the ROI level, cannabis users showed reduced FA in the left insula connections to the occipital fusiform gyrus (medial and lateral subdivisions) and the posterior lingual gyrus. Edge-wise testing further identified a single left-hemispheric insula–occipital connection with higher RD in cannabis users, although this effect was based on a reduced per-edge sample size due to missing tract estimates.

The insula's role as an integrative hub for linking sensory information with interoceptive and affective salience processing is confirmed by tractography studies and is consistent with the anatomical and functional capacity of occipito-insular projections (44). The fusiform and lingual regions contribute to ventral visual-stream functions (what processing stream), suggesting that altered microstructural organization within these pathways could reflect differences in how visually derived information is coupled to salience and motivational circuitry – potentially relevant for cue-driven attention in cannabis use (45). The effects observed in the occipital region were modest in comparison to the findings related to the insula and limbic systems. Furthermore, these effects exhibited a left-lateralized pattern and demonstrated sensitivity to the availability of neural tracts as well as the non-specificity of diffusion metrics. It is essential to replicate these findings in larger sample sizes and to utilize diffusion imaging techniques that are optimized for long-range, crossing-fiber pathways in order to draw more robust mechanistic inferences.

Endocannabinoid system (eCS)

In a large longitudinal adolescent cohort, Albaugh and colleagues showed that cannabis use was associated with accelerated age-related cortical thinning (predominantly prefrontal) from ages 14 to 19, and that the spatial pattern of cannabis-related thinning was significantly associated with a PET-derived map of CB1 receptor availability (2). This suggests an essential developmental mechanism that exogenous cannabinoids (particularly Δ9-THC) may disrupt normative endocannabinoid signaling during periods of rapid cortical maturation, with disproportionate effects in CB1-rich regions already undergoing substantial developmental thinning.

Manza et al. examined cannabis dependence in a large Human Connectome Project sample and reported cortical thickness and density differences (most prominently in the precuneus) along with white matter FA reductions in specific bundles, supporting this receptor map evidence.(46) Critically, they linked the spatial pattern of cortical thinning to the regional expression of monoacylglycerol lipase (MAGL), a principal enzyme that regulates 2-AG signaling. Together, these studies support a model in which cortical and white matter differences in cannabis dependence are not randomly distributed but instead align with neurochemical features of endocannabinoid signaling and metabolism.

According to this framework, our findings of focal insular thinning, reduced OFC volume, and altered insula–amygdala microstructure can be interpreted as a network-level expression of endocannabinoid-linked vulnerability in circuits that couple interoception (insula), valuation (OFC), and affective salience and stress processing (amygdala). This is consistent with the emphasis placed by ENIGMA on CB1-rich, addiction-relevant ROIs, including insula, OFC, and amygdala, even though specific regional effects can vary by sample and dependence status (19).

The insula's role in salience detection and network switching also provides a plausible neurophysiological link to clinical phenotypes observed in chronic cannabis use, including altered cue reactivity, motivational salience assignment, and impairments in cognitive control under affective load (34, 40). Although our study did not include functional connectivity, prior work in other substance-using populations has shown that salience network structural integrity (notably insula–ACC pathways) can have complex, sometimes non-linear relationships with cognitive performance and exposure burden. This leads to a key hypothesis for

future cannabis research: insular thinning and selective insula–limbic tract alterations may serve as a structural substrate for dysregulated salience processing, potentially contributing to the transition from recreational to compulsive use.

Limitations

The sample size and cross-sectional design of the study can be noted as limitations. The cohort (n = 26) limits the power to detect minor effects and increases susceptibility to sampling variability. Cross-sectional contrasts cannot establish causality. However, longitudinal studies indicate that baseline thickness did not predict later cannabis use, supporting the plausibility of cannabis-associated cortical change (47).

Tractography and diffusion metric specificity. DTI-derived FA, MD, AD, and RD are non-specific proxies for microstructure, and streamline-based tractography is affected by ROI geometry, crossing fibers, partial volume effects, and algorithmic biases – issues that are especially relevant for deep structures such as the insula. Therefore, interpretation of “lower MD” or “higher FA” should remain at the level of altered microstructural organization rather than as a direct claim about myelination or axonal density.

Several insula–subcortical connections could not be reliably estimated in all participants, reducing per-edge sample sizes and potentially biasing edge-wise results toward more consistently tracked tracts. This limitation reinforces the need for replication in larger samples and with diffusion acquisitions optimized for subcortical tracking.

Detailed characterization of cannabis potency (THC/CBD ratio), age of onset, abstinence duration, and co-use of nicotine or alcohol is essential for mechanistic inference and was not leveraged here to model dose–response relationships. Large-scale efforts (e.g., ENIGMA) suggest that dependence status and sex may moderate OFC and cerebellar findings; these moderators should be explicitly tested in future insula-centered analyses. However, these studies, which had heterogeneous samples, where alcohol use may drive cerebellar or white matter changes(48). Due to the restriction applied to historically pure controls and users with no comorbidities other than nicotine, our findings of insula thinning are more likely to be a direct result of cannabis exposure rather than alcohol induced neurotoxicity or other confounding factors.

Conclusions

This study provides evidence that chronic cannabis use in young adults is associated with volume reductions in the global gray matter, brainstem, amygdala, thalamus, cerebellar cortex, and orbitofrontal cortex; robust bilateral insular cortical thinning observed at both whole-insula and parcel-wise resolution; higher FA and lower diffusivity indices in left insula-amygdala; and lower FA in right insula–hippocampus, right insula–precentral gyrus, left insula-occipital pathways involving ventral occipital regions (Fusiform and Lingual gyri). These results align with recent evidence that cannabis-related cortical thinning patterns correspond to CB1 receptor distribution and endocannabinoid metabolic biology, supporting an endocannabinoid-linked vulnerability model for structural alterations in insula-centered salience and valuation circuits.

Future work should prioritize larger, well-phenotyped samples; longitudinal designs spanning adolescence into adulthood; multi-shell diffusion and advanced microstructural modeling (e.g., free-water, NODDI, fixel-based metrics); and integration with functional connectivity and behavioral measures of interoception, cue reactivity, and cognitive control. These approaches will be critical for determining whether insular thinning and alterations in insula–limbic tracts represent consequences of chronic exposure, predisposing vulnerabilities, compensatory adaptations, or a combination of these that varies across developmental stage and dependence severity.

Declarations

Ethical Approval and consent to participate

All research procedures were approved by the Ethical Committee of Kashan University of Medical Sciences and Health Services and were conducted in accordance with the Declaration of Helsinki. The study protocol was approved according to the code of ethics of the IR.KAUMS.MEDNT.REC.1401.015. Written informed consent was obtained from all subjects.

Consent for publication

Not applicable. This study does not contain data from any individual person (no case reports, images, or videos of identifiable individuals).

Availability of data and materials

The datasets generated and analyzed during the current study are available from the corresponding author upon reasonable request.

Competing interests

The authors declare that they have no competing interests.

Funding

This study was funded by Kashan University of Medical Sciences and Health Services (research number: 400158). The funder had no role in study design, data collection, analysis, interpretation, or the decision to submit for publication.

Authors' contributions

F.M.F. and R.S. wrote the main manuscript text. R.S. prepared the original draft and carried out data collection. F.M.F. performed the image analysis, data curation, and statistical analysis. N.J. was responsible for image acquisition and contributed to image analysis. M.A.A. and A.G. supervised the study. All authors contributed to conceptualization and methodology. F.M.F., M.A.A., and N.J. reviewed and edited the manuscript. All authors reviewed the final manuscript.

Acknowledgments

We are grateful to Clinical Research Development Unit Matini /Kargarnejad Hospitals, Kashan University of Medical Sciences, Kashan, Iran, for granting us funding that supported our study (ID: 400158; Ethics ID: IR.KAUMS.MEDNT.REC.1401.015). We would also like to thank the National Brain Mapping Laboratory for image acquisition, and of course, we thank all the volunteers of our study who gave their time to make this study possible. In Addition, authors would like to thank the Clinical Research Development Unit of Kashan Shahid Beheshti Hospital and Clinical Research Development Unit Matini /Kargarnejad Hospitals, Kashan University of Medical Sciences, Kashan, Iran. The authors also express their sincere gratitude to the Narcotics Control Headquarters of Isfahan Province for their collaborative efforts and unwavering assistance in conducting this study.

References

1. UNODC. World drug report 2025. 2025.
2. Albaugh MD, Ottino-Gonzalez J, Sidwell A, Lepage C, Juliano A, Owens MM, et al. Association of cannabis use during adolescence with neurodevelopment. 2021;78(9):1031–40.
3. Gowin JL, Ellingson JM, Karoly HC, Manza P, Ross JM, Sloan ME, et al. Brain Function Outcomes of Recent and Lifetime Cannabis Use. JAMA Netw Open. 2025;8(1):e2457069.
4. Hirjak D, Schmitgen MM, Werler F, Wittemann M, Kubera KM, Wolf ND, et al. Multimodal MRI data fusion reveals distinct structural, functional and neurochemical correlates of heavy cannabis use. Addict Biol. 2022;27(2):e13113.
5. Zehra A, Burns J, Liu CK, Manza P, Wiers CE, Volkow ND, et al. Cannabis Addiction and the Brain: a Review. J Neuroimmune Pharmacol. 2018;13(4):438–52.
6. Ertl N, Freeman TP, Mokrysz C, Ofori S, Borissova A, Petrilli K, et al. Acute effects of different types of cannabis on young adult and adolescent resting-state brain networks. Neuropsychopharmacology. 2024;49(10):1640–51.
7. Delvecchio G, Oldani L, Mandolini GM, Pigoni A, Ciappolino V, Schiena G, et al. Brain morphology of cannabis users with or without psychosis: A Pilot MRI study. 2020;2020(162):1–20.
8. Damasio AJN. Mental self: The person within. 2003;423(6937):227–.
9. Li C, Pang X, Shi K, Long Q, Liu J, Zheng JJFiN. The insula is a hub for functional brain network in patients with anti-N-methyl-D-aspartate receptor encephalitis. 2021;15:642390.
10. Menon V, Uddin LQJBs, function. Saliency, switching, attention and control: a network model of insula function. 2010;214(5):655–67.
11. Naqvi NH, Bechara AJTWHotCNoA. The Insula: A Critical Neural Substrate for Drug Seeking under Conflict and Risk. 2015:128–50.
12. Ghaziri J, Tucholka A, Girard G, Boucher O, Houde J-C, Descoteaux M, et al. Subcortical structural connectivity of insular subregions. 2018;8(1):8596.
13. Battistella G, Fornari E, Annoni J-M, Chtioui H, Dao K, Fabritius M, et al. Long-term effects of cannabis on brain structure. 2014;39(9):2041–8.

14. Koenders L, Cousijn J, Vingerhoets WA, Van Den Brink W, Wiers RW, Meijer CJ, et al. Grey matter changes associated with heavy cannabis use: a longitudinal sMRI study. 2016;11(5):e0152482.
15. Koenis MM, Durnez J, Rodrigue AL, Mathias SR, Alexander-Bloch AF, Barrett JA, et al. Associations of cannabis use disorder with cognition, brain structure, and brain function in African Americans. 2021;42(6):1727–41.
16. Mackey S, Allgaier N, Chaarani B, Spechler P, Orr C, Bunn J, et al. Mega-analysis of gray matter volume in substance dependence: general and substance-specific regional effects. 2019;176(2):119–28.
17. Chye Y, Suo C, Lorenzetti V, Batalla A, Cousijn J, Goudriaan AE, et al. Cortical surface morphology in long-term cannabis users: A multi-site MRI study. 2019;29(2):257–65.
18. Gilman JM, Kuster JK, Lee S, Lee MJ, Kim BW, Makris N, et al. Cannabis use is quantitatively associated with nucleus accumbens and amygdala abnormalities in young adult recreational users. 2014;34(16):5529–38.
19. Lorenzetti V, Gaillard A, Mctavish E, Grace S, Rossetti MG, Batalla A, et al. Cannabis dependence is associated with reduced hippocampal subregion volumes independently of sex: findings from an ENIGMA Addiction Working Group Multi-Country Study. 2024;9(6):e1565–e78.
20. Robinson EA, Gleeson J, Arun AH, Clemente A, Gaillard A, Rossetti MG, et al. Measuring white matter microstructure in 1,457 cannabis users and 1,441 controls: a systematic review of diffusion-weighted MRI studies. 2023;2:1129587.
21. Livny A, Cohen K, Tik N, Tsarfaty G, Rosca P, Weinstein AJEn. The effects of synthetic cannabinoids (SCs) on brain structure and function. 2018;28(9):1047–57.
22. Sarollahi R, Ghaderi A, Banafshe HR, Atlasi MAJIJoHRB, Addiction. Lifetime, last month and excessive prevalence of addictive substances consumption among the general population and university students in the city of Tehran. 2025;14(3).
23. Fischl BJN. FreeSurfer. 2012;62(2):774–81.
24. McGrath H, Zaveri HP, Collins E, Jafar T, Chishti O, Obaid S, et al. High-resolution cortical parcellation based on conserved brain landmarks for localization of multimodal data to the nearest centimeter. 2022;12(1):18778.
25. Ghaziri J, Tucholka A, Girard G, Houde J-C, Boucher O, Gilbert G, et al. The corticocortical structural connectivity of the human insula. 2017;27(2):1216–28.
26. Makris N, Rushmore R, Kaiser J, Albaugh M, Kubicki M, Rathi Y, et al. A proposed human structural brain connectivity matrix in the Center for Morphometric Analysis Harvard-Oxford Atlas Framework: a historical perspective and future direction for enhancing the precision of human structural connectivity with a novel neuroanatomical typology. 2023;45(4):161–80.
27. Jenkinson M, Beckmann CF, Behrens TE, Woolrich MW, Smith SMJN. Fsl. 2012;62(2):782–90.
28. Tournier J-D, Smith R, Raffelt D, Tabbara R, Dhollander T, Pietsch M, et al. MRtrix3: A fast, flexible and open software framework for medical image processing and visualisation. 2019;202:116137.
29. Avants BB, Tustison NJ, Song G, Cook PA, Klein A, Gee JCJN. A reproducible evaluation of ANTs similarity metric performance in brain image registration. 2011;54(3):2033–44.

30. Fonov VS, Evans AC, McKinstry RC, Almli CR, Collins DJN. Unbiased nonlinear average age-appropriate brain templates from birth to adulthood. 2009;47:S102.
31. Xu H, Li J, Huang H, Yin B, Li DD. Abnormal developmental of structural covariance networks in young adults with heavy cannabis use: a 3-year follow-up study. Transl Psychiatry. 2024;14(1):45.
32. Batalla A, Bhattacharyya S, Yuecel M, Fusar-Poli P, Crippa JA, Nogue S, et al. Structural and functional imaging studies in chronic cannabis users: a systematic review of adolescent and adult findings. 2013;8(2):e55821.
33. Rocchetti M, Crescini A, Borgwardt S, Caverzasi E, Politi P, Atakan Z, et al. Is cannabis neurotoxic for the healthy brain? A meta-analytical review of structural brain alterations in non-psychotic users. 2013;67(7):483–92.
34. Filbey FM, Aslan S, Calhoun VD, Spence JS, Damaraju E, Caprihan A, et al. Long-term effects of marijuana use on the brain. 2014;111(47):16913–8.
35. Lorenzetti V, Chye Y, Silva P, Solowij N, Roberts CAJEaop, neuroscience c. Does regular cannabis use affect neuroanatomy? An updated systematic review and meta-analysis of structural neuroimaging studies. 2019;269(1):59–71.
36. Cao Z, Ottino-Gonzalez J, Cupertino RB, Schwab N, Hoke C, Catherine O, et al. Mapping cortical and subcortical asymmetries in substance dependence: Findings from the ENIGMA Addiction Working Group. 2021;26(5):e13010.
37. Chye Y, Mackey S, Gutman BA, Ching CR, Batalla A, Blaine S, et al. Subcortical surface morphometry in substance dependence: An ENIGMA addiction working group study. 2020;25(6):e12830.
38. Battistella G, Fornari E, Annoni JM, Chtioui H, Dao K, Fabritius M, et al. Long-term effects of cannabis on brain structure. Neuropsychopharmacology. 2014;39(9):2041–8.
39. Battistella G, Fornari E, Thomas A, Mall JF, Chtioui H, Appenzeller M, et al. Weed or wheel! FMRI, behavioural, and toxicological investigations of how cannabis smoking affects skills necessary for driving. PLoS One. 2013;8(1):e52545.
40. Droutman V, Read SJ, Bechara AJTics. Revisiting the role of the insula in addiction. 2015;19(7):414–20.
41. Soleimani N, Kazemi K, Helfroush MS, Aarabi AJSR. Altered brain structural and functional connectivity in cannabis users. 2023;13(1):5847.
42. Cousijn J, Toenders YJ, van Velzen LS, Kaag AMJAb. The relation between cannabis use, dependence severity and white matter microstructure: A diffusion tensor imaging study. 2022;27(1):e13081.
43. Shura RD, Hurley RA, Taber KH. Insular cortex: structural and functional neuroanatomy. The Journal of neuropsychiatry. 2014;26(4):iv–282.
44. Cerliani L, Thomas RM, Jbabdi S, Siero JC, Nanetti L, Crippa A, et al. Probabilistic tractography recovers a rostrocaudal trajectory of connectivity variability in the human insular cortex. 2012;33(9):2005–34.
45. Pessoa L, Kastner S, Ungerleider LGJCBR. Attentional control of the processing of neutral and emotional stimuli. 2002;15(1):31–45.
46. Manza P, Yuan K, Shokri-Kojori E, Tomasi D, Volkow ND. Brain structural changes in cannabis dependence: association with MAGL. Molecular psychiatry. 2020;25(12):3256–66.

47. Li W, Xu C, Xu H, Yin B, Xu H, Li DJAB. Abnormal Cortical Thickness Development in Young Adults With Heavy Cannabis Use: A Longitudinal Study. 2025;30(5):e70040.
48. Rossetti MG, Mackey S, Patalay P, Allen NB, Batalla A, Bellani M, et al. Sex and dependence related neuroanatomical differences in regular cannabis users: findings from the ENIGMA Addiction Working Group. Transl Psychiatry. 2021;11(1):272.

Figures

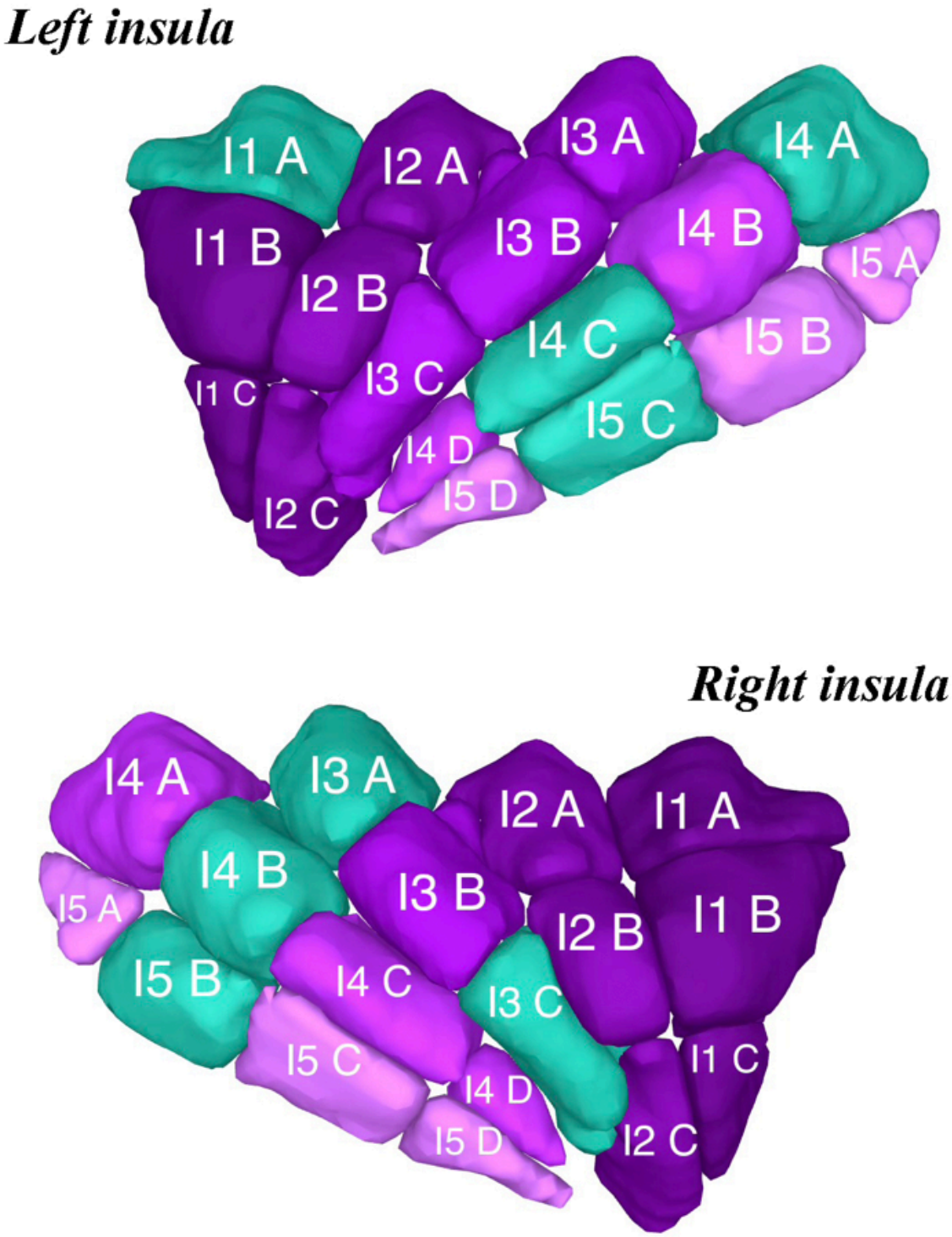

Figure 1

YBA three-dimensional insula parcellation with titles, showing parcels with significant thickness differences between the groups of the study in green.

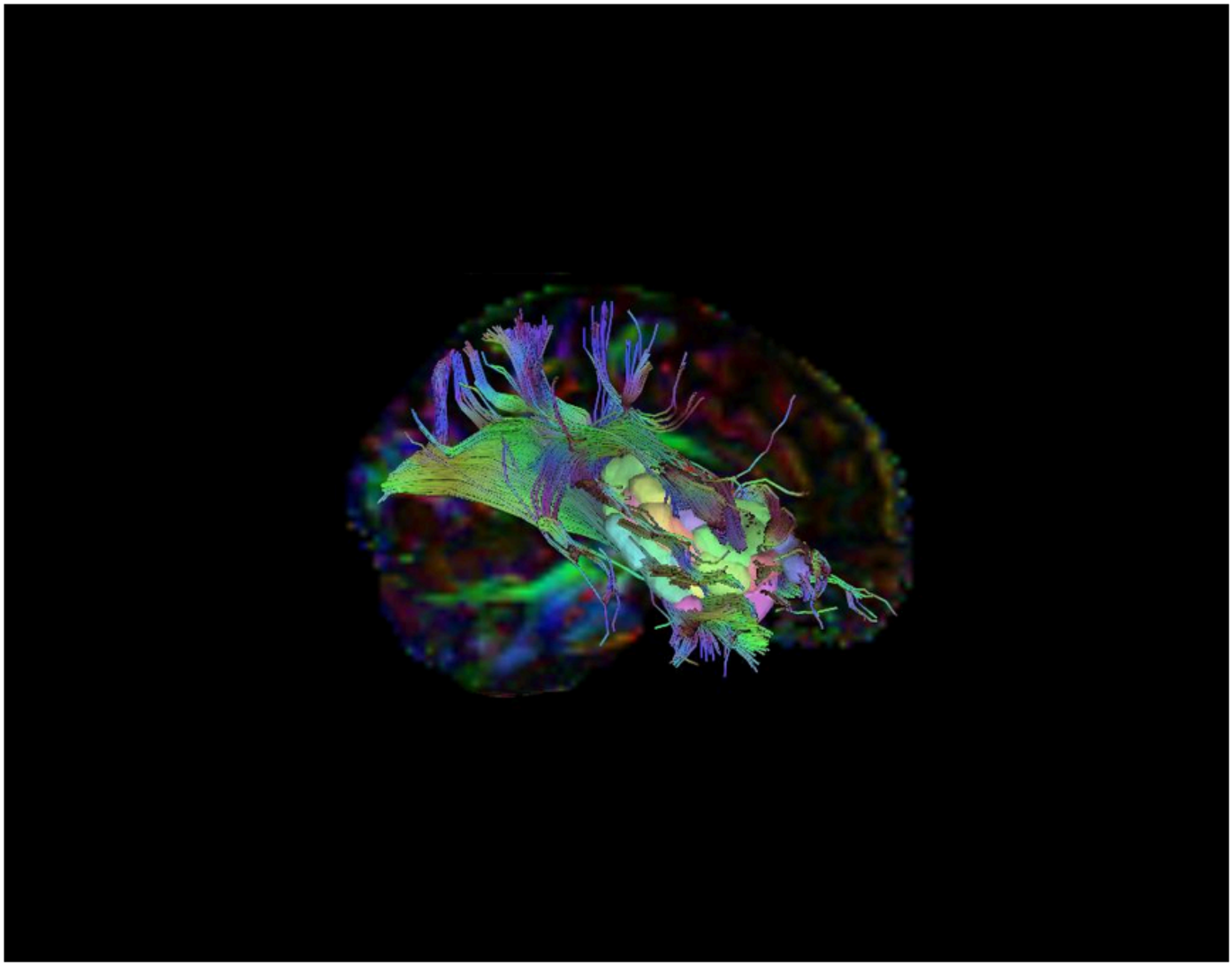

Figure 2

Diffusion MRI tractography demonstrating structural connectivity of the right insular cortex with surrounding cortical and subcortical regions. Streamlines were reconstructed using high-angular-resolution diffusion imaging (HARDI)–based tractography and overlaid on a sagittal anatomical brain image. Color-coded fibers represent the principal diffusion orientations, highlighting the complex white-matter architecture associated with the insular connectome.